

1 Glassy state molecular mobility and its relationship  
2 to the physico-mechanical properties of plasticized  
3 hydroxypropyl methylcellulose (HPMC) films.

4 Samuel K. Owusu-Ware\*<sup>2</sup>, Joshua S. Boateng<sup>1</sup>, Babur Z. Chowdhry<sup>1</sup>, and Milan D.  
5 Antonijevic\*<sup>1</sup>.

6 <sup>1</sup> School of Science, Faculty of Engineering and Science, University of Greenwich (Medway  
7 Campus), Chatham Maritime, Kent ME4 4TB, UK.

8 <sup>2</sup> AstraZeneca, Macclesfield, Cheshire, SK10 2NA

9 **Corresponding Authors:**

10 \*E-mail: Samuel.owusu-ware@astrazeneca.com

11 \*E-mail: M.Antonijevic@greenwich.ac.uk

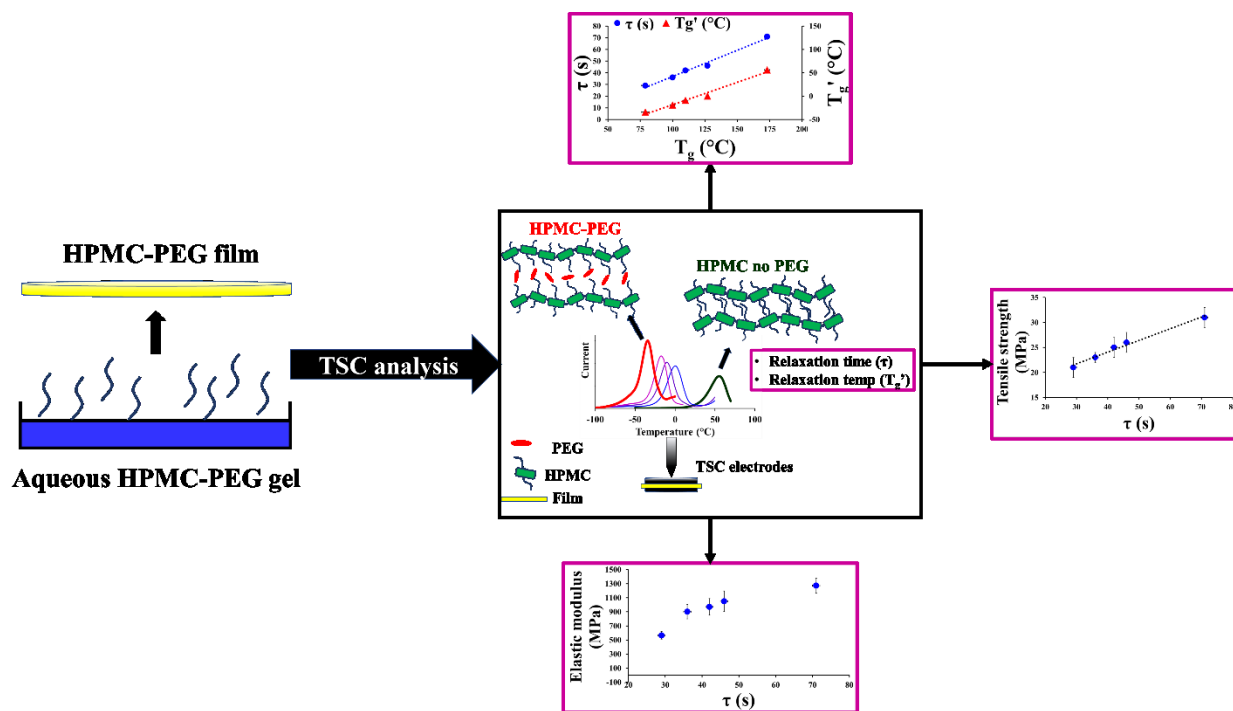
12 **ABSTRACT**

13 Changes in tensile properties and the glass transition temperature ( $T_g$ ) of plasticized polymer films  
14 are typically attributed to molecular mobility, often with no empirical data to support such an  
15 assertion. Here solvent cast HPMC films containing varying amounts of PEG, as the plasticizer,  
16 were used to assess the dependence of tensile properties and the  $T_g$  on glassy state molecular  
17 mobility. Parameters of molecular mobility (molecular relaxation time and temperature) were  
18 determined by Thermally Stimulated Current Spectroscopy (TSC). The tensile properties and  $T_g$   
19 of the HPMC films were determined by Texture Analyzer and DSC, respectively. Molecular  
20 mobility detected by TSC were cooperative and occurred at temperatures ( $T_g'$ ) well below (113 to  
21 127°C below) the bulk  $T_g$ . The relaxation times ( $\tau$ ) were  $71 \pm 1$ ,  $46 \pm 1$ ,  $42 \pm 1$ ,  $36 \pm 1$  and  $29 \pm 1$   
22 s for HPMC films containing 0, 6, 8, 11 and 17 % (w/w) PEG, respectively. The  $T_g$  and glassy  
23 state molecular mobility were found to be intimately linked and demonstrated a linear dependence.  
24 While tensile strength was found to be linearly related to molecular relaxation time, tensile  
25 elongation and elastic modulus exhibited a non-linear dependence on molecular mobility. The data  
26 presented in this work demonstrates the complex nature of the relationship between plasticizer  
27 content, molecular mobility,  $T_g$  and tensile properties for plasticized polymeric films. It highlights  
28 that the dependence of the bulk physico-mechanical properties on glassy state molecular mobility,  
29 differ greatly. Therefore, empirical characterization of molecular mobility is important to fully  
30 understand and predict the thermo-mechanical behavior of plasticized polymer films. This work  
31 demonstrates the unique capability of TSC to provide key information on molecular mobility and  
32 its influence on bulk level properties of materials. Data generated from TSC proves useful for  
33 stability and performance ranking, in addition to the ability to predict materials behavior using

34 data generated at or below typical storage conditions in the pharmaceutical, food, and polymer  
35 industries.

36

### 37 GRAPHICAL ABSTRACT



38

39

40

41

### 42 KEYWORDS:

43 Thermally stimulated current spectroscopy (TSC)

44 Molecular mobility

45 Mechanical properties

46 Relaxation time

47 Polymer films

48 Capsules

49 Glass transition

50

## 51 **1.0 INTRODUCTION**

52 Hydroxypropylmethyl cellulose (HPMC), also known as hypromellose, is a cellulose based  
53 synthetic polymer that is considered safe for human consumption, and has broad application in the  
54 food and pharmaceutical industries (Burdock, 2007, Shit and Shah, 2014). As an excipient, HPMC  
55 functions as a thickener, binder, bio-adhesive or solubility enhancer (Jaya et al., 2012; Chowdary  
56 et al., 2014; Huichao et al., 2014). HPMC also possesses good film forming properties and is a  
57 common excipient in pharmaceutical film formulations including film coated tablets (Missaghi  
58 and Fassihi, 2006; Al-Tabakha, 2010; Karki et al., 2016,). The use of HPMC as an alternative to  
59 gelatin in capsule formulations has been of interest, as it offers distinct advantages. For example,  
60 it is of a vegetable source and therefore by-passes the stringent regulations imposed on the use of  
61 materials of animal origin in pharmaceutical products by regulators (Ku et al., 2011). This  
62 advantage over gelatin has been a key driver for the development of HPMC based capsules i.e.  
63 Vegicaps Soft (Catalent Pharma Solutions) and hard capsules such as Vcaps Plus (Capsugel)  
64 (Missaghi and Fassihi, 2006; Ku et al., 2011).

65

66 An important characteristic of any capsule or film-based product is their ability to withstand  
67 mechanical damage and exhibit the appropriate level of flexibility (Al-Tabakha, 2010; Curtis-Fisk  
68 et al., 2012) to enable easy handling and processing. The characterization of mechanical properties  
69 and the ability to predict the influence of formulation parameters on these properties is therefore  
70 important in the development of polymer films for pharmaceutical applications.

71  
72 Mechanical properties of films are typically described by tensile strength, elongation and elastic  
73 (Young's) modulus. These properties are commonly measured by means of uni-axial tensile stress  
74 testing, on a section of isolated film. It is well established that the measured mechanical properties  
75 of a piece of film are influenced by temperature and plasticizer concentration. For example,  
76 polymers exhibit stiff/brittle behavior at temperatures below the glass transition temperature ( $T_g$ ),  
77 while at temperatures above the  $T_g$ , they are flexible/ductile materials (Smith et al., 2009, Karki et  
78 al., 2016) and may even flow. Plasticizers are key components for optimizing mechanical  
79 properties in film formulations. Increasing the amount of plasticizer enhances flexibility,  
80 workability or distensibility by reducing the melt viscosity. This is typically associated with the  
81 lowering of the  $T_g$  and elastic modulus (Honary and Orafai, 2002; Daniels, 2009). In addition, the  
82 molecular weight of plasticizers has also been shown to be a factor in plasticizer efficiency  
83 (Honary and Orafai, 2002).

84  
85 Several theories exist, explaining the mechanism by which plasticizers change thermal and  
86 mechanical properties of polymeric films. The most widely known are the lubricity, gel and free  
87 volume theories (Daniels, 2009; Marcilla and Beltran, 2017). While details of these theories are  
88 beyond the scope of this article, it is important to note that each theory implies that the degree of  
89 motional freedom in plasticized materials is the most essential property governing thermo-  
90 mechanical behavior.

91  
92 Various analytical techniques have been employed to investigate molecular mobilities in polymer  
93 films. Techniques such as de-wetting (Connie and John, 2005, Wang and McKenna, 2013),

94 ellipsometry (Tress et al., 2010, Inoue et al., 2009, Mok et al., 2010), neutron scattering (Inoue et  
95 al., 2009, Soles et al., 2002, Soles et al., 2003, Clough et al., 2011), fluorescence spectroscopy  
96 (Connie and John, 2005, Roth et al., 2007, Priestley et al., 2007, Kim et al., 2008), X-ray  
97 reflectivity (Wallace et al., 1995, Weber et al., 2001), Brillouin light scattering (Forrest et al., 1997,  
98 Mattsson et al., 2000, Fukao et al., 2001), secondary ion mass spectroscopy (Zheng et al., 1997,  
99 Pu et al., 2001, Connie and John, 2005) and dielectric spectroscopy (Priestley et al., 2007, Yin et  
100 al., 2012, Yin et al., 2013, Tress et al., 2010, Serghei et al., 2005) have all been used to interrogate  
101 the molecular mobility characteristics in polymer films. These studies have often been focused on  
102 motional dynamics at varying thickness of polymer films on a solid support or free-standing.  
103 Collectively, these studies provide a wealth of information on molecular mobility at small  
104 thickness scales. Whilst this is important and provides interesting information on mobility of  
105 confined polymers for several fields of application i.e. microelectronic, optoelectronics and  
106 biological sensors (Pique et al., 2003, Hojati-Talemi et al., 2013), they do not address the  
107 relationship between molecular mobility and the bulk properties of polymer films for  
108 pharmaceutical applications. Furthermore, empirical studies in the literature investigating the  
109 direct relationship between parameters of glassy state molecular mobility, and thermo-mechanical  
110 properties of polymer films are scarce, and therefore require investigation.

111  
112 In this work Thermally Stimulated Current (TSC), a relatively simple dielectric analysis technique,  
113 was employed to characterize molecular mobility in the glassy amorphous state of plasticized  
114 HPMC films. An attempt is made to relate the parameters of molecular mobility (ease and rate of  
115 mobility) to the tensile properties of the plasticized films and the  $T_g$ .

116

117 Details of the TSC technique can be found elsewhere (Turnhout, 1975; Ramos and Mano, 1997;  
118 Correia et al., 2000; Owusu-Ware et al., 2013). Briefly, TSC measures currents generated by the  
119 movement of molecular dipoles, as a function of temperature, in response to externally applied  
120 static electrical field. The external electrical field polarizes molecules in the material i.e. causing  
121 bonds, atoms and whole/segments of molecules to align against an externally applied electrical  
122 field. This polarization is “frozen-in” by quench cooling to a temperature well below the  
123 temperature of polarization, at which point the external electrical field is removed. During heating,  
124 the “frozen-in” polarizations relax (depolarize) i.e. molecules, parts of molecules, and dipoles  
125 move back to their native orientations, generating measurable currents. The shape, size and  
126 temperature of the current signal is dependent on the type of relaxation, the rate and the ease with  
127 which the different activated relaxations occur, in addition to the fraction of molecules undergoing  
128 relaxation. This makes it possible to characterize the distinct types of molecular dipole relaxations  
129 (molecular mobilities) in polymer films i.e.  $\alpha$ -relaxation that is associated with the glass transition  
130 and the subtler secondary relaxations ( $\beta$  and  $\gamma$  type relaxations). Since the current generated is  
131 proportional to the externally applied electrical field, the sensitivity of the instrument can be  
132 controlled by the operator. Furthermore, TSC is known to have better resolution and sensitivity to  
133 the different modes/types of molecular relaxation when compared with dielectric spectroscopy  
134 analysis (DEA) and dynamic mechanical analysis (DMA) (Saffell et al., 1991; Grein et al., 2004;  
135 Ramos et al., 2004; Barker and Antonijevic, 2011).

136

137 There are two main experiments that can be performed, namely Thermally Stimulated  
138 Depolarization Current (TSDC) and Thermal Windowing (TW) (Turnhout, 1975). In TSDC  
139 experiments the sample is simply polarized at a defined temperature (the polarization temperature

140 ( $T_p$ ) for a time (polarization time ( $t_p$ )) long enough to obtain equilibrium saturation of the various  
141 molecular orientations in the material. This is then ‘frozen in’ by cooling to a temperature ( $T_0$ )  
142 well below the  $T_p$  before a linear heating ( $\beta$ ) is applied from  $T_0$  to a final temperature ( $T_f$ ) that is  
143 higher than the  $T_p$ .

144

145 The second experiment, the TW, deconvolutes the complex TSDC signal into its various discrete  
146 relaxation modes (those that have different relaxation times and activation energies). Here, a  
147 narrow temperature window of polarization ( $T_w$ ) is applied covering the entire width of global  
148 TSDC signal. Each polarization is followed with a depolarization step, where the relaxation modes  
149 with the fastest relaxation time is removed from the system by cooling the sample to a few degrees  
150 below the initial polarization temperature ( $T_d$ ). At this point, the external electrical field is short  
151 circuited as the sample is held isothermal for a brief time ( $t_w$ ). The remaining slower relaxations  
152 are ‘frozen in’ on cooling and relax back to their native orientation upon heating. The discrete  
153 relaxation processes detected are used to generate a map of relaxation times and enthalpy of  
154 activation by means of the Eyring kinetic model fitting, which are then used to determine the types  
155 of relaxations exhibited by the material under investigation.

156

## 157 **2.0 EXPERIMENTAL**

### 158 **2.1 Materials**

159 Hydroxypropyl methylcellulose (HPMC) (average molecular weight  $\sim$  860 kDa, viscosity of 1%  
160 aqueous solution at 20°C is  $\sim$ 145 mPa.s) and PEG 400 were purchased from Sigma Aldrich  
161 (Gillingham, UK).

162



## 163 **2.2 Methods**

### 164 **2.2.1 Preparation of films**

165 Films were prepared using the solvent casting method. Aqueous gels (2 % w/w) consisting of 0,  
166 6, 8, 11 and 17 % w/w PEG 400 were prepared in deionized water (heated to 60°C) and the mixture  
167 stirred at ambient temperature overnight (~18 hours in total). 50 g of the gel was poured into a  
168 plastic Petri dish (diameter of 140 mm) and left in a 60°C oven for 24 hours. The resultant films  
169 were stored in a desiccator over silica for two days before analyzing. The films that were optically  
170 clear with no visible defects were chosen for analysis. The thickness of the films was determined  
171 using a digital caliper and found to be  $0.047 \pm 0.001$  mm. XRPD analysis was performed and  
172 showed the films to be completely amorphous.

173

### 174 **2.2.2 Thermogravimetric analysis (TGA)**

175 TGA studies were performed using the Q5000 IR (TA Instruments, UK). Sample mass of  $3.2 \pm$   
176  $0.5$  mg was used for all compounds. Samples were subjected to a heat-cool-heat experiment under  
177 a nitrogen atmosphere at a flow rate of 25 ml/min in hermetically sealed Tzero aluminium pans  
178 with a single pin hole in the lid. Each sample was heated from ambient temperature to 150°C at a  
179 heating rate of 10°C/min, cooled back to 25°C and reheated to 150°C at 10°C/min.

180

### 181 **2.2.3 Differential scanning calorimetry (DSC)**

182 DSC studies were performed with a Q2000 (TA Instruments, UK) under a nitrogen atmosphere at  
183 a flow rate of 50 mL/min, using hermetically sealed Tzero aluminium pans with a pin hole in the  
184 lid. Sample mass of  $2.60 \pm 0.24$  mg was heated to 140 °C to remove moisture, equilibrated at -  
185 90 °C, held isothermally for 5 minutes and heated to 200 °C at 10 °C/min.

186

#### 187 **2.2.4 Texture analysis**

188 Mechanical (tensile) properties of the HPMC films were analyzed at ambient temperature with a  
189 TA HD plus (Stable Micro System, UK) texture analyzer. The films ( $n = 3$ ) devoid of any visible  
190 physical defects were cut into dumb-bell shapes. A trigger force of 0.1 N was applied during the  
191 testing and the films stretched between two tensile grips at a speed of 0.2 mm/s to a maximum  
192 distance of 300 mm or until the films broke. The % elongation at break, the tensile strength and  
193 elastic modulus were determined (Lim and Hoag, 2013).

194

#### 195 **2.2.5 Thermally stimulated current (TSC) experiments**

196 TSC studies using the thermally stimulated depolarization current (TSDC) experiment, covering  
197 the range -100 to 70 °C were conducted with a TSCII/RMA spectrometer (SETARAM, France)  
198 equipped with a 900 series LN2 (Liquid Nitrogen) micro-dosing cooling system (Norhof,  
199 Netherlands) and 6517A electrometer (Keithley, USA). Experiments were performed using  
200 electrode arrangement that consists of bottom (13 mm diameter) and upper (10 mm diameter) steel  
201 electrodes. The sample diameter of the film cut for analysis was  $12.0 \pm 0.5$  mm and the surface  
202 area of the sample in direct contact between the top and the bottom electrode was  $78.54 \text{ mm}^2$ . The  
203 analysis chamber was evacuated to  $10^{-4}$  mbar and flushed several times with high purity helium  
204 (1.1 bar) prior to analysis. Each sample was initially subjected to a pre-treatment in which it was  
205 heated to 60 °C (the film forming temperature) and held isothermal for 30 min. This was followed  
206 by evacuation of the analysis chamber to  $10^{-4}$  bar and flushing three times with high purity helium  
207 (1.1 bars). The global TSDC signals were obtained by polarizing the sample at 60, 5, -5, -12, and  
208 -30 °C for films containing 0, 6, 8, 11, and 17 % w/w PEG 400, respectively, using polarization

209 field ( $E_p$ ) ranging from 50 to 250 V/mm in increments of 50 V/mm for 2 min ( $t_p$ ). In the case of  
210 thermal windowing experiments (TW), samples were polarized with  $E_p = 250$  V/mm at  $T_p$  at 2 to  
211 65 °C, -60 to 33 °C, -60 to 39 °C, -60 to 9 °C and -72 to -12 °C for films containing 0, 6, 8, 11 and  
212 17 % PEG 400, respectively, in increments of 3 °C. The temperature range chosen ensured that  
213 the thermal windowing experiments covered the whole temperature range of the global TSDC  
214 signal.  $T_w$  was set at 3 °C, whilst  $t_p$  and  $t_w$  were set at 2 min for all four samples.

215

### 216 **3.0 RESULTS and DISCUSSION**

#### 217 **3.1 TGA and DSC**

218 All samples analyzed (HPMC and HPMC with different percentage of PEG) were found to lose 4  
219 - 6 % moisture when heated from ambient temperature to 150 °C and this dehydration process  
220 occurred below 120 °C, which was the removal of free water. As shown in Figure 1, the second  
221 heating profile was practically flat, indicating complete removal of water from the films when  
222 heated to 150 °C.

223

224 The DSC data presented in Figure 2 showed that the bulk  $T_g$  of the films decreased with increasing  
225 PEG content, which is typical behavior of polymeric films (Khodaverdi et al., 2012). The decrease  
226 in  $T_g$  as a function of PEG content in the HPMC films is non-linear i.e. a sharper decrease in  $T_g$   
227 was observed from 0 to 8 % PEG, beyond this point the magnitude of the change in  $T_g$  as a function  
228 of PEG decreases, with the plot moving towards a plateau. This demonstrates that beyond a certain  
229 PEG content (% w/w) the efficiency of plasticization decreases and therefore greater amount of  
230 PEG is required to cause further decrease in the  $T_g$ .

231

232 One of the most important influences of plasticizers on the glass transition process observed in  
233 DSC, and often disregarded, is the decrease in the steepness and increase in the width of the glass  
234 transition process. This occurs because plasticizers reduce the energy difference between the  
235 glassy and rubbery phase by facilitating increased degree of molecular mobility i.e. molecules of  
236 plasticized films in the glassy state exhibit increasingly higher state of mobility and therefore  
237 kinetic energy, with increasing plasticizer content. This presents a problem in detecting  $T_g$  of  
238 plasticized films, as the energy change associated with the glass transition process becomes too  
239 small to detect by DSC. Khodaverdi and colleagues (2012) highlighted this problem in their  
240 investigation comparing different plasticizers and their effect on thermo-responsive properties of  
241 Eudragit RS films. In their work  $T_g$  data could not be provide for Eudragit RS film plasticized with  
242 20 % triethyl citrate (TEC) plasticizer, because it could not be detected on the DSC. This impacts  
243 the ability to make direct comparison between two or more plasticizers with different plasticization  
244 efficiency across a broad range of concentrations/ % content. In these situations, TSC is perhaps  
245 one of the most useful technique to use to overcome such issues (Antonijevic et al., 2008).

246

### 247 **3.2 Texture Analysis**

248 The data obtained from the texture analysis are presented in Table 1. The results obtained were  
249 consistent with what is generally expected for a plasticized polymeric film. Increasing plasticizer  
250 concentration increased elongation at break, whilst the tensile strength and elastic modulus  
251 decreased.

252

253 **Table 1.** Summary of the tensile strength, percent elongation at break and elastic modulus of  
254 HPMC films with increasing PEG 400 (% w/w) content.

% PEG content (w/w)	Tensile strength (MPa)	% Elongation at break	Elastic modulus (MPa)
0	31 ± 2	4 ± 1	1271 ± 105
6	26 ± 2	8 ± 2	1050 ± 147
8	25 ± 2	9 ± 3	971 ± 117
11	23 ± 1	11 ± 3	903 ± 104
17	21 ± 2	23 ± 1	565 ± 54

255  
256 Elongation is the extendibility of the film from the initial length to the point of break and it  
257 quantifies the flexibility/ stretchability of films. The increase in elongation observed as a function  
258 of plasticizer concentration, can be explained by the reduction in inter-molecular attractive forces  
259 between HPMC molecules (Lim and Hoag, 2013). This disruption of the strong interactions  
260 between HPMC molecules by the PEG molecules reduces rigidity and increases flexibility of the  
261 film by promoting HPMC polymer chain mobility. Replacement of strong intermolecular  
262 interactions between HPMC molecules by weaker HPMC-PEG interactions also explains the  
263 decrease in the tensile strength observed as PEG concentration increased. Elastic modulus  
264 measures the resistance of the film to elastic deformation, and provides information on the film  
265 stiffness/strength (Lim and Hoag, 2013). This was also found to decrease with increasing  
266 plasticizer concentration, which was expected.

267

### 268 **3.3 Thermally Stimulated Depolarization Current (TSDC)**

269 For this study only the initial global TSDC peak detected for each sample was considered. There  
270 were two main reasons for excluding signals beyond the initial global TSDC peak; firstly, it was

271 found that the current signal generated after the initial relaxation process (first peak) appears to  
272 increase infinitely in each sample (examples provided in section B of the supplementary). In these  
273 situations, it was not possible to decipher contributions from molecular dipole relaxations and  
274 movement of other charged species. Secondly the first peak had similar shape and was consistent  
275 across all samples. It was therefore considered to originate from the same type of relaxations,  
276 which enabled direct comparison between the samples analyzed.

277  
278 The current signal generated from TSDC experiments can arise from the movement of various  
279 charged species, originating from several polarization mechanisms i.e. electronic, atomic, space  
280 charge, interfacial and molecular dipole polarization (Ibar, 1993, Turnhout, 1975). When  
281 investigating parameters associated with molecular mobility, it is important to ascertain that the  
282 TSDC output is due to molecular dipole relaxations. To determine this, samples were analyzed  
283 several times with increasing electrical field strengths. In the case of a molecular dipole relaxation,  
284 a linear relationship should exist between the ratios of the applied electrical field strength and the  
285 total polarization (P) (area under the TSDC signal) (Correia et al., 2000, Diogo et al., 2008, Pinto  
286 et al., 2010).

287  
288 The TSDC signals obtained for the samples analyzed proved to originate from molecular dipole  
289 relaxations i.e. linear regression of the ratio of applied electrical field strength against the ratio of  
290 the polarization generated, yielded  $r^2$  values  $> 0.994$  and a slope close to unity ( $>0.91 < 1.1$ ), for all  
291 samples analyzed. Hence the TSDC profile obtained in this study represent the relaxation/mobility  
292 of polarized HPMC and PEG molecules. Figure 3 shows typical output of these TSDC  
293 experiments. Increasing PEG concentration (% w/w) was found to decrease the temperature of

294 molecular dipole relaxation (Figure 4). The relaxation peak temperature ( $T_m$ ) of the un-plasticized  
295 HPMC film was detected at  $56.0 \pm 0.7$  °C, whilst films containing 6, 8, 11 and 17 % (w/w) PEG  
296 were observed at  $-0.3 \pm 0.8$  °C,  $-9.0 \pm 1.1$  °C,  $-18.6 \pm 1.4$  °C and  $-33.8 \pm 1.0$  °C, respectively. The  
297 results also showed increased intensity/size of relaxation current generated with increasing PEG  
298 content. These findings showed that the addition of PEG to HPMC films both enhanced the  
299 amount/extent of molecular mobility and the ease with which mobility occurred in the glassy state.  
300 A plot of PEG content and the  $T_m$  was found to follow a similar profile to that observed between  
301 PEG content and the  $T_g$  determined by DSC (Figure 5) i.e. an initial, relatively sharp decrease in  
302  $T_m$  with increase in PEG content up to 8 %, from which point the change in  $T_m$  as a function of  
303 PEG content decreases, tending towards a plateau. This demonstrates that molecular mobility, well  
304 below the glass transition process, and the  $T_g$  itself are influenced in a similar way by PEG and  
305 supports the idea that glassy state molecular mobility and the bulk glass transition process are  
306 intimately linked.

307

### 308 **3.4 Thermal windowing (TW) results**

309 The application of the thermal windowing experiments deconvoluted the complex global  
310 relaxation peak into discrete relaxation processes. As shown in Figure 6, all the PEG plasticized  
311 HPMC films exhibit two groups of discrete relaxation processes within temperature range of  
312 analysis. The first group (lower temperature grouping) corresponds to the global relaxation process  
313 identified in the TSDC investigations. The second group of relaxations were part of the infinitely  
314 increasing TSDC signal (section B of the supplementary). It was not possible to assess the  
315 existence of this second group of relaxations for the HPMC films with no PEG as heating these  
316 samples above 70°C was suspected to cause a change to the nature of the material (and hence

317 mobility) in subsequent experiments. Both groups of discrete relaxation processes, only identified  
318 in the HPMC films containing PEG, increased with increasing PEG content. However, the relative  
319 intensity of the second group of discrete relaxation processes (relative to the first group of discrete  
320 relaxation processes) appeared to increase more in line with the increase in PEG concentration.  
321 This implied that this group of relaxations mostly originated from the movement of PEG  
322 molecules, and were assigned to the increased number of mobile dipoles in PEG molecules  
323 compared to HPMC molecules. The current signals associated with these processes were very  
324 noisy and inconsistent, due to contributions from space and interfacial charges. As a result, it did  
325 not form part of the discussion in this work.

326  
327 The inserts in Figure 6 show the distribution of relaxation times ( $\tau$ ), referred to as the Bucci lines,  
328 for each discrete relaxation process. Straight Bucci lines generally indicate narrowly distributed  
329 activation energies, and imply a single mode of molecular relaxation e.g. twisting of polymer end  
330 group or orientation of a single fragment of the polymer chain. Bucci line curvature, on the other  
331 hand, suggests activation energies are not narrowly distributed, therefore each ‘discrete’ relaxation  
332 process may in fact contain two or more different modes of molecular orientations (Alvarez et al.,  
333 2000; Correia et al., 2000; Diogo and Ramos, 2008; Viciosa et al., 2010). This suggests activation  
334 of two or more groups of molecular fragments with different activation energies. In this study the  
335 Bucci lines obtained for the first group of relaxation processes, were generally found to be straight.  
336 Each Bucci line was fitted with the Eyring equation to determine the enthalpy of activation ( $\Delta H^\ddagger$   
337 ), entropy of activation ( $\Delta S^\ddagger$ ) and Gibbs free energy of activation ( $\Delta G^\ddagger$ ). More details on the  
338 determination of these parameters along with the relaxation time ( $\tau$ ) are provided in section A of  
339 the supplementary.



340

341 The cooperativity of these isolated relaxation processes was investigated by overlaying the  
342 enthalpy of activation ( $\Delta H^\ddagger$ ) with zero-entropy predictions in a Starkweather type analysis  
343 (Ramos and Mano, 1997) as shown in Figure 7. In this analysis the assumption is made that  $\Delta H^\ddagger$   
344 values have no entropic contribution ( $\Delta S^\ddagger = 0$ ) when the relaxation process is non-cooperative.  
345 For cooperative relaxation processes, the  $\Delta H^\ddagger$  value is assumed to have an entropic contribution  
346 ( $\Delta S^\ddagger \neq 0$ ) and will therefore deviate from the zero-entropy prediction line.

347

348 The Starkweather analysis provides a means to differentiate between non-cooperative secondary  
349 relaxations ( $\beta$ - and  $\gamma$ -relaxations) and the cooperative primary relaxations ( $\alpha$ -relaxation). The un-  
350 plasticized HPMC films and the PEG plasticized HPMC films were found to deviate from the zero-  
351 entropy predictions, which implied that the molecular relaxation processes identified in each film  
352 corresponded to a cooperative relaxation process (cooperative molecular mobility).

353

354 It is expected that for cooperative mobility to occur in these films, the backbone of the HPMC  
355 polymer molecule would have to move, which would require the cooperative  
356 movement/orientation of neighboring HPMC and PEG molecules, causing a cascade of molecular  
357 orientations throughout the material. This would typically be associated with high enough energy  
358 that is detectable in DSC experiments. This level of cooperativity was observed at higher  
359 temperatures ( $>70$  °C) for these materials by DSC. The fact that the cooperative relaxations in the  
360 TSC studies were not detected in the DSC suggests that they were of too low energy and may  
361 originate from small groups of HPMC polymer segments in localized regions of the film (Owusu-  
362 Ware et al., 2016). That is, small groups of polymer segments that do not cause significant

363 viscous/heat changes in the bulk material to generate a sufficiently large signal to be detected by  
364 DSC. These low energy cooperative relaxations are likely to arise mostly from the orientation of  
365 the hydroxypropyl methyl side chains and small units of the HPMC end groups, facilitated by the  
366 cooperative orientation of PEG molecules. The TSDC peak temperature ( $T_m$ ) of these cooperative  
367 molecular relaxations is denoted  $T_g'$  from here on.

368  
369 Cooperative molecular relaxations or  $\alpha$ -relaxations, are typically associated with the bulk glass  
370 transition and expected to be present at or near the  $T_g$  (Ramos and Mano, 1997; Ramos et al., 2004;  
371 Smith and Bedrov, 2007; Diogo and Ramos, 2008; Pinto et al., 2010). Data presented in this study  
372 demonstrates that this is not the case for all materials. For the HPMC films analyzed, cooperative  
373 mobility occurs well below the  $T_g$  (between 113 to 127 °C below the  $T_g$ ) where localized, low  
374 energy molecular relaxations occur. Such information is pertinent for understanding stability  
375 implications of plasticized drug loaded polymeric films, where such mobility could result in  
376 polymer-drug phase separation and/or crystallization of an amorphous drug dispersions.  
377 Furthermore, understanding molecular mobility in materials at temperatures below or around their  
378 storage conditions can allow for a better prediction of stability and performance ranking, in  
379 addition to offering opportunity to optimize materials performance at the molecular level.

380

### 381 **3.5 Relationships between molecular mobility, $T_g$ and mechanical properties**

382 The molecular relaxation time ( $\tau$ ),  $T_g'$  and the  $T_g$  for the samples analyzed are presented in Table  
383 2. The relaxation time determined in this study is a measure of the time scale of the cooperative  
384 molecular relaxations associated with the  $T_g'$ , and is therefore a direct measure of molecular

385 mobility in the glassy state. The fact that both  $T_g'$  and  $\tau$  decreased with increasing PEG content,  
386 demonstrates that PEG enhances the ease and rate of molecular mobility in the HPMC films.

387

388 **Table 2** Data for the cooperative relaxation TSDC peak temperature ( $T_g'$ ), relaxation time ( $\tau$ ), for  
389 the highest intensity TW output, and bulk glass transition tempetaure ( $T_g$ ) obtained for the HPMC  
390 films.

% PEG content (w/w)	$T_g'$ (°C)	$T_g$ (°C)	$\tau$ (s)
0	$56 \pm 1$	$173 \pm 2$	$71 \pm 1$
6	$0 \pm 1$	$127 \pm 1$	$46 \pm 1$
8	$-9 \pm 1$	$110 \pm 2$	$42 \pm 1$
11	$-19 \pm 1$	$100 \pm 2$	$36 \pm 1$
17	$-34 \pm 1$	$79 \pm 3$	$29 \pm 1$

391

392 The influence of plasticizers on  $T_g$  and tensile properties is typically linked to molecular mobility,  
393 usually with no empirical evidence. As such, the nature of the relationship between mobility,  $T_g$   
394 and tensile parameters is not always clear. Data generated from TSC in this study have identified  
395 several important trends between molecular mobility and physico-mechanical properties. For  
396 example,  $\tau$  and  $T_g'$  were found to be linearly related to  $T_g$  (Figures 8). The lower the  $\tau$  or  $T_g'$  the  
397 lower the  $T_g$ , and vice versa. This shows that mobility at low temperature regions of the glassy  
398 amorphous films (TSC data), are directly related to the glass transition process observed at a much  
399 higher temperature in DSC.

400

401 The tensile strength of the plasticized HPMC films was also found to be linearly related to  $\tau$  i.e.,  
402 tensile strength increases as  $\tau$  increases (Figure 9). Tensile elongation was found to decrease with  
403 increasing  $\tau$ , while the elastic modulus increased with increasing  $\tau$  in a non-linear fashion for both  
404 parameters (Figures 10 and 11). This again demonstrates a clear link between values obtained for  
405 molecular mobility (TSC data) and mechanical properties. Materials with lower molecular  
406 relaxation times will have lower resistance to imposed stress i.e. they are able to easily and quickly  
407 respond to the uniaxial tensile deformation stress, resulting in lower tensile strength and greater  
408 tensile elongation. On the other hand, materials with higher molecular relaxation times will exhibit  
409 greater resistance to the imposed uniaxial deformation stress, as they are stiffer and unable to  
410 follow imposed stress as easily/quickly as those with lower molecular relaxation times. The link  
411 between parameters of molecular mobility as measured by TSC and the mechanical properties,  
412 defined by tensile analysis, point out that materials with lower relaxation times are likely to exhibit  
413 greater flexibility when subjected to brief and low stresses. However, they will easily succumb to  
414 increasing and prolonged stresses, and are likely to quickly change from elastic to plastic  
415 deformation.

416

417 The increase in tensile strength and elastic modulus, and decrease in tensile elongation as a  
418 function of  $\tau$ , demonstrates that these localized segmental mobilities observed in the TSC, are  
419 major contributors to the mechanical properties of plasticized HPMC films. It is shown that  
420 decreasing molecular relaxation time, by means of plasticizer, reduces the stiffness parameter  
421 (elastic modulus) and the strength of the film. Decreasing relaxation time i.e. increase rate of  
422 molecular mobility, is also an indication of increased degrees of motional freedom for the HPMC  
423 molecules. This is caused by the disruption of the stronger HPMC inter-molecular interactions by

424 PEG molecules, which in turn limits closer packing of the HPMC molecules, resulting in increased  
425 free volume, making it easy for molecules to slip past each other. It is by this same process that  
426 the tensile strength and elastic modulus are also reduced.

427

428 The trends observed demonstrate the complexity of the relationships between molecular mobility  
429 and tensile properties. The knowledge gained from these relationships provide opportunities to  
430 understand and potentially optimize polymer films, but also highlights challenges associated with  
431 optimizing mechanical properties of film based formulations. Since the interdependence of the  
432 parameters of tensile properties of plasticized HPMC films on mobility differ, it is possible to  
433 optimize the tensile property of interest at the molecular level. However, the ability to do this is  
434 challenging, since it is not possible to change one parameter without impacting another with  
435 completely different dependence on the magnitude of change. For example, below a  $\tau$  value of 45  
436 s, a small change in  $\tau$  is accompanied with a sharper change in tensile elongation and elastic  
437 modulus compared to tensile strength.

#### 438 4.0 Conclusions

439 TSC has been used to characterize the glassy state molecular mobility of HPMC polymer films,  
440 with varying levels of PEG content (0 – 17 % w/w). PEG was shown to decrease the molecular  
441 relaxation temperature and time. The mobility observed in these films was of a cooperative nature.  
442 This was unexpected given that the relaxations observed were so far below the  $T_g$ , and had such  
443 low heat energy associated, that they could not be detected by DSC. Such an observation  
444 demonstrates, for the HPMC films, that considerable molecular mobility exists well below room  
445 temperature, which can have major physical and chemical stability implications. The relationship  
446 between molecular relaxation parameters ( $T_g'$  and  $\tau$ ),  $T_g$  and tensile properties have been  
447 empirically demonstrated. It was found that  $T_g$  was linearly related to molecular relaxation time  
448 ( $\tau$ ) and the  $T_g'$  (relaxation peak temperature) with an  $r^2$  of  $> 0.97$ . It has been shown that increasing  
449 molecular relaxation time within the glassy state decreases the  $T_g$ . Tensile strength was also found  
450 to be linearly related to molecular relaxation time with an  $r^2$  value  $> 0.98$ , in which increasing  
451 molecular relaxation time increased tensile strength. A completely different relationship was  
452 observed for tensile elongation and elastic modulus. These two mechanical parameters had a non-  
453 linear relationship with molecular relaxation time. Increasing molecular relaxation time decreases  
454 tensile elongation until a certain point (45 s), where further increase in relaxation time has little  
455 impact on elongation. Similar behavior was observed for elastic modulus, except in this case elastic  
456 modulus increased with molecular relaxation time.

457

458 The data presented in this work empirically demonstrates the complex nature of the relationship  
459 between molecular mobility,  $T_g$  and tensile properties for plasticized HPMC films. Whilst these  
460 findings agree with the general inference that increased molecular mobility is the cause of decrease

461 in  $T_g$ , tensile strength and elastic modulus and the increase in elongation for plasticized polymeric  
462 films, it highlights that the dependence of these bulk parameters on molecular mobility differ  
463 greatly. Therefore, empirical measurement of molecular mobility parameters is important to fully  
464 understand and predict the thermo-mechanical behavior of polymeric films. TSC has proved to be  
465 a vital technique in characterizing glassy state molecular mobility. Knowledge gained from this  
466 technique is very useful for stability and performance ranking, and offers the opportunity to predict  
467 materials behavior using data generated at or below typical storage conditions.

468

#### 469 **Acknowledgement**

470 This study was funded by the University of Greenwich. Samuel K Owusu-Ware wishes to thank  
471 the University of Greenwich for funding Post-Doctoral research.

472 **5.0 References**

- 473 Al-Tabakha, M. M. (2010) 'HPMC capsules: current status and future prospects', *J Pharm Pharm Sci*, 13(3),  
474 pp. 428-42.
- 475 Alvarez, C., Correia, N. T., Ramos, J. J. M. and Fernandes, A. C. (2000) 'Glass transition relaxation and  
476 fragility in a side-chain liquid crystalline polymer: a study by TSDC and DSC', *Polymer*, 41, pp.  
477 2907-2914.
- 478 Antonijevic, M. D., Craig, D. Q. M. and Barker, S. A. (2008) 'The role of space charge formation in the  
479 generation of thermally stimulated current (TSC) spectroscopy data for a model amorphous  
480 system', *International Journal of Pharmaceutics*, 353, pp. 8-14.
- 481 Barker, S. and Antonijevic, M. D. (2011) 'Thermal analysis-Dielectric techniques', in Storey, R.A. & Ymen,  
482 I. (eds.) *Solid State Characterization of Pharmaceutics*. United Kingdom: WILEY, pp. 187-204.
- 483 Burdock, G. A. (2007) 'Safety assessment of hydroxypropyl methylcellulose as a food ingredient', *Food  
484 Chem Toxicol*, 45(12), pp. 2341-51.
- 485 Chowdary, Y. A., Raparla, R. and Madhuri, M. (2014) 'Formulation and Evaluation of Multilayered Tablets  
486 of Pioglitazone Hydrochloride and Metformin Hydrochloride', *J Pharm (Cairo)*, 2014, pp. 848243.
- 487 CLOUGH, A., PENG, D. D., YANG, Z. H. & TSUI, O. K. C. 2011. Glass Transition Temperature of  
488 Polymer Films That Slip. *Macromolecules*, 44, 1649-1653.
- 489 CONNIE, B. R. & JOHN, R. D. 2005. Mobility on Different Length Scales in Thin Polymer Films. In:  
490 DUTCHER, J. R. & MARANGONI, A. G. (eds.) *Soft Materials: Structure and Dynamics*. New  
491 York: Marcel Dekker.
- 492 Correia, N. T., Alvarez, C., Ramos, J. J. M. and Descamps, M. (2000) 'Molecular motions in molecular  
493 glasses as studied by thermally stimulated depolarization currents (TSDC)', *Chemical Physics*, 252,  
494 pp. 151-163.
- 495 Curtis-Fisk, J., Sheskey, P., Balwinski, K., Coppens, K., Mohler, C. and Zhao, J. (2012) 'Effect of  
496 formulation conditions on hypromellose performance properties in films used for capsules and  
497 tablet coatings', *AAPS PharmSciTech*, 13(4), pp. 1170-8.
- 498 Daniels, P. H. (2009) 'A Brief Overview of Theories of PVC Plasticization and Methods Used to Evaluate  
499 PVC-Plasticizer Interaction', *JOURNAL OF VINYL & ADDITIVE TECHNOLOGY*, pp. 5.
- 500 Diogo, H. P. and Ramos, J. J. (2008) 'Slow molecular mobility in the crystalline and amorphous solid states  
501 of glucose as studied by thermally stimulated depolarization currents (TSDC)', *Carbohydrate  
502 Research*, 343, pp. 2797-2803.
- 503 Diogo, H. P., Pinto, S. S. and Moura Ramos, J. J. (2008) 'Relaxation behaviour of d(-)-salicin as studied by  
504 Thermally Stimulated Depolarisation Currents (TSDC) and Differential Scanning Calorimetry  
505 (DSC)', *International Journal of Pharmaceutics*, 358(1-2), pp. 192-197.
- 506 FORREST, J. A., DALNOKIVERESS, K. & DUTCHER, J. R. 1997. Interface and chain confinement  
507 effects on the glass transition temperature of thin polymer films. *Physical Review E*, 56, 5705-  
508 5716.
- 509 Grein, C., Bernreitner, K. and Gahleitner, M. (2004) 'Potential and Limits of Dynamic Mechanical Analysis  
510 as a Tool for Fracture Resistance Evaluation of Isotactic Polypropylenes and Their Polyolefin  
511 Blends', *Journal of Applied Polymer Science*, 93, pp. 1854-1867.
- 512 HOJATI-TALEMI, P., BAECHLER, C., FABRETTO, M., MURPHY, P. & EVANS, D. 2013. Ultrathin  
513 Polymer Films for Transparent Electrode Applications Prepared by Controlled Nucleation. *ACS  
514 Applied Materials & Interfaces*, 5, 11654-11660.
- 515 Honary, S. and Orafi, H. (2002) 'The effect of different plasticizer molecular weights and concentrations  
516 on mechanical and thermomechanical properties of free films', *Drug Dev Ind Pharm*, 28(6), pp.  
517 711-5.
- 518 Huichao, W., Shouying, D., Yang, L., Ying, Y. and Di, W. (2014) 'The application of biomedical polymer  
519 material hydroxy propyl methyl cellulose(HPMC) in pharmaceutical preparations', *Journal of  
520 Chemical and Pharmaceutical Research*, 6(5), pp. 6.
- 521 Ibar, J. P. (1993) *Fundamentals of thermal stimulated current and relaxation map analysis*. SLP Press.



522 INOUE, R., KANAYA, T., NISHIDA, K., TSUKUSHI, I., TELLING, M. T. F., GABRYS, B. J., TYAGI,  
523 M., SOLES, C. & WU, W. L. 2009. Glass transition and molecular mobility in polymer thin films.  
524 *Physical Review E*, 80, 031802.

525 Jaya, S., Chowdary, K. P. R. and Rao, P. (2012) 'Effect of Binders on the Dissolution Rate and Dissolution  
526 Efficiency of Ritonavir Tablets', *International Research Journal of Pharmaceutical and Applied  
527 Sciences*, 2(4), pp. 5.

528 Karki, S., Kim, H., Na, S.-J., Shin, D., Jo, K. and Lee, J. (2016) 'Thin films as an emerging platform for  
529 drug delivery', *Asian Journal of Pharmaceutical Sciences*, 11(5), pp. 559-574.

530 Khodaverdi, E., Tekie, F.S.M., Amoli, S.S., Sadeghi, F. (2012) 'Comparison of Plasticizer Effect on  
531 Thermo-responsive Properties of Eudragit RS Films' *AAPS Pharmaceutical Science and  
532 Technology*, 13 (3), pp. 1024-1030.

533 KIM, J., SANDOVAL, R. W., DETTMER, C. M., NGUYEN, S. T. & TORKELESON, J. M. 2008.  
534 Compatibilized polymer blends with nanoscale or sub-micron dispersed phases achieved by  
535 hydrogen-bonding effects: Block copolymer vs blocky gradient copolymer addition. *Polymer*, 49,  
536 2686-2697.

537 Ku, M. S., Lu, Q., Li, W. and Chen, Y. (2011) 'Performance qualification of a new hypromellose capsule:  
538 Part II. Disintegration and dissolution comparison between two types of hypromellose capsules',  
539 *Int J Pharm*, 416(1), pp. 16-24.

540 Lim, H. and Hoag, S. W. (2013) 'Plasticizer Effects on Physical–Mechanical Properties of Solvent Cast  
541 Soluplus® Films', *AAPS PharmSciTech*, 14(3), pp. 903-910.

542 Marcilla, A. and Beltran (2017) *Handbook of Plasticizers*. 3rd edn. Toronto: ChemTech Publishing, p. 119-  
543 129.

544 Missaghi, S. and Fassihi, R. (2006) 'Evaluation and comparison of physicommechanical characteristics of  
545 gelatin and hypromellose capsules', *Drug Dev Ind Pharm*, 32(7), pp. 829-38.

546 MOK, M. M., KIM, J., MARROU, S. R. & TORKELESON, J. M. 2010. Ellipsometry measurements of glass  
547 transition breadth in bulk films of random, block, and gradient copolymers. *European Physical  
548 Journal E*, 31, 239-252.

549 Owusu-Ware, S. K., Boateng, J., Jordan, D., Portefaix, S., Tasseto, R., Ramano, C. D. and Antonijević, M.  
550 D. (2016) 'Molecular mobility of hydroxyethyl cellulose (HEC) films characterised by thermally  
551 stimulated currents (TSC) spectroscopy', *Int J Pharm*, 497(1-2), pp. 222-7.

552 Owusu-Ware, S. K., Chowdhry, B. Z., Leharne, S. A. and Antonijevic, M. D. (2013) 'Novel analytical  
553 approaches for the study of mobility and relaxation phenomena in positional isomers of GABA',  
554 *Physical Chemistry Chemical Physics*, 15(46), pp. 20046-20053.

555 Pinto, S. S., Diogo, H. P., Nunes, T. G. and Moura Ramos, J. J. (2010) 'Molecular mobility studies on the  
556 amorphous state of disaccharides. I--thermally stimulated currents and differential scanning  
557 calorimetry', *Carbohydrate Research*, 345(12), pp. 1802-1807.

558 PIQUE, A., AUYEUNG, R. C. Y., STEPNOWSKI, J. L., WEIR, D. W., ARNOLD, C. B., MCGILL, R. A.  
559 & CHRISEY, D. B. 2003. Laser processing of polymer thin films for chemical sensor applications.  
560 *Surface & Coatings Technology*, 163, 293-299.

561 PRIESTLEY, R. D., RITTIGSTEIN, P., BROADBELT, L. J., FUKAO, K. & TORKELESON, J. M. 2007.  
562 Evidence for the molecular-scale origin of the suppression of physical ageing in confined polymer:  
563 fluorescence and dielectric spectroscopy studies of polymer-silica nanocomposites. *Journal of  
564 Physics-Condensed Matter*, 19.

565 PU, Y., RAFAILOVICH, M. H., SOKOLOV, J., GERSAPPE, D., PETERSON, T., WU, W. L. &  
566 SCHWARZ, S. A. 2001. Mobility of polymer chains confined at a free surface. *Physical Review  
567 Letters*, 87.

568 Ramos, J. J. M. and Mano, J. F. (1997) 'Some comments on the significance of the compensation effect  
569 observed in thermally stimulated current experiments', *Polymer*, 38(5), pp. 1081-1089.

570 Ramos, J. J. M., Correia, N. T. and Diogo, H. P. (2004) 'Vitrification, nucleation and crystallization in  
571 phenyl-2-hydroxybenzoate (salol) studied by Differential Scanning Calorimetry (DSC) and

572 Thermally Stimulated Depolarisation Currents (TSDC)', *Physical Chemistry Chemical Physics*,  
573 6(4), pp. 793-798.

574 ROTH, C. B., MCNERNY, K. L., JAGER, W. F. & TORKELSON, J. M. 2007. Eliminating the enhanced  
575 mobility at the free surface of polystyrene: Fluorescence studies of the glass transition temperature  
576 in thin bilayer films of immiscible polymers. *Macromolecules*, 40, 2568-2574.

577 Saffell, J. R., Matthiesen, A., McIntyre, R. and Ibar, J. P. (1991) 'Comparing thermal stimulated current  
578 (TSC) with other thermal analytical methods to characterise the amorphous phase of polymers',  
579 *Thermochimica Acta*, 192, pp. 243-264.

580 SERGHEI, A., MIKHAILOVA, Y., HUTH, H., SCHICK, C., EICHHORN, K. J., VOIT, B. & KREMER,  
581 F. 2005. Molecular dynamics of hyperbranched polyesters in the confinement of thin films.  
582 *European Physical Journal E*, 17, 199-202.

583 Shit, S. C. and Shah, P. M. (2014) 'Edible Polymers: Challenges and Opportunities', *Journal of Polymers*,  
584 2014, pp. 13.

585 Smith, G. D. and Bedrov, D. (2007) 'Relationship between the  $\alpha$ - and  $\beta$ -relaxation processes in amorphous  
586 polymers: Insight from atomistic molecular dynamics simulations of 1,4-polybutadiene melts and  
587 blends', *Journal of Polymer Science Part B: Polymer Physics*, 45(6), pp. 627-643.

588 Smith, K. E., Sawicki, S., Hyjek, M. A., Downey, S. and Gall, K. (2009) 'The effect of the glass transition  
589 temperature on the toughness of photopolymerizable (meth)acrylate networks under physiological  
590 conditions', *Polymer (Guildf)*, 50(21), pp. 5112-5123.

591 SOLES, C. L., DOUGLAS, J. F., WU, W. L. & DIMEO, R. M. 2002. Incoherent neutron scattering and the  
592 dynamics of confined polycarbonate films. *Physical Review Letters*, 88.

593 SOLES, C. L., DOUGLAS, J. F., WU, W. L. & DIMEO, R. M. 2003. Incoherent neutron scattering as a  
594 probe of the dynamics in molecularly thin polymer films. *Macromolecules*, 36, 373-379.

595 TRESS, M., ERBER, M., MAPESA, E. U., HUTH, H., MULLER, J., SERGHEI, A., SCHICK, C.,  
596 EICHHORN, K. J., VOLT, B. & KREMER, F. 2010. Glassy Dynamics and Glass Transition in  
597 Nanometric Thin Layers of Polystyrene. *Macromolecules*, 43, 9937-9944.

598 Turnhout, J. (1975) *Thermally stimulated discharge of polymer electrets*. Netherland: Elsevier Scientific  
599 Publishing Company, p. 1-65.

600 Viciosa, M. T., Ramos, J. J. M. and Diogo, H. P. (2010) 'Molecular dynamics of an epoxy resin  
601 studied by Thermally Stimulated Depolarisation Currents', *Journal of Non-Crystalline  
602 Solids*, 356(50-51), pp. 2858-2864.

603 WALLACE, W. E., VANZANTEN, J. H. & WU, W. L. 1995. INFLUENCE OF AN IMPENETRABLE  
604 INTERFACE ON A POLYMER GLASS-TRANSITION TEMPERATURE. *Physical Review E*,  
605 52, R3329-R3332.

606 WANG, J. H. & MCKENNA, G. B. 2013. Viscoelastic and Glass Transition Properties of Ultrathin  
607 Polystyrene Films by Dewetting from Liquid Glycerol. *Macromolecules*, 46, 2485-2495.

608 WEBER, R., ZIMMERMANN, K. M., TOLAN, M., STETTNER, J., PRESS, W., SEECK, O. H.,  
609 ERICHSEN, J., ZAPOROJTCHEKOV, V., STRUNSKUS, T. & FAUPEL, F. 2001. X-ray  
610 reflectivity study on the surface and bulk glass transition of polystyrene. *Physical Review E*, 64.

611 YIN, H. J., NAPOLITANO, S. & SCHONHALS, A. 2012. Molecular Mobility and Glass Transition of  
612 Thin Films of Poly(bisphenol A carbonate). *Macromolecules*, 45, 1652-1662.

613 YIN, H., CANGIALOSI, D. & SCHONHALS, A. 2013. Glass transition and segmental dynamics in thin  
614 supported polystyrene films: The role of molecular weight and annealing. *Thermochimica Acta*,  
615 566, 186-192.

## 617 List of Figures

618 **Figure 1.** A typical overlay of TGA thermograms obtained for the first and second heating of  
619 HPMC films with varying PEG contents.

620 **Figure 2.** A plot showing the relationship between  $T_g$  and PEG content (% w/w) of the HPMC-  
621 PEG films.

622  
623 **Figure 3.** TSDC signals obtained with increasing electrical field strength ( $E_p$ ) for HPMC films in  
624 the absence of PEG. The insert shows the linear relationship between the ratios of electrical field  
625 strength and polarisation (P) for the HPMC films (no PEG).

626  
627 **Figure 4.** TSDC molecular relaxation signals obtained using an electrical field strength ( $E_p$ ) of  
628 250 V/mm for HPMC films containing 0, 6, 8, 11 and 17 % (w/w) PEG 400.

629  
630 **Figure 5.** A plot showing the relationship between TSDC  $T_m$  and PEG content (% w/w) of the  
631 HPMC-PEG films.

632  
633 **Figure 6.** TW output showing the discrete relaxation processes obtained for (a) un-plasticised  
634 HPMC films and HPMC films containing (b) 6 %, (c) 8 %, (d) 11 % and (e) 17 % (w/w) PEG 400.  
635 The inserts display the Bucci lines obtained for each discrete relaxation process.

636  
637 **Figure 7.** Overlay of the plots of the enthalpy of activation ( $\Delta H^\ddagger$ ) values for the discrete  
638 relaxation process and the zero-entropy prediction ( $\Delta S^\ddagger = 0$ ) obtained for un-plasticised HPMC  
639 films and HPMC films containing 6 %, 8 %, 11 % and 17 % (w/w) PEG 400.

640  
641 **Figure 8.** The relationship between the bulk glass transition temperature ( $T_g$ ), the cooperative  
642 relaxation peak temperatures ( $T_g'$ ) and molecular relaxation times associated with the  $T_g'$  for  
643 HPMC polymer films containing 0, 6, 8, 11 and 17 % (w/w) PEG.

644  
645 **Figure 9.** A plot of the relationship between tensile strength and molecular relaxation time ( $\tau$ ) for  
646 the HPMC-PEG films.

647  
648 **Figure 10.** A plot of the relationship between tensile elongation and molecular relaxation time ( $\tau$ )  
649 for the HPMC-PEG films.

650  
651 **Figure 11.** A plot of the relationship between elastic modulus and molecular relaxation time ( $\tau$ )  
652 for the HPMC-PEG films.

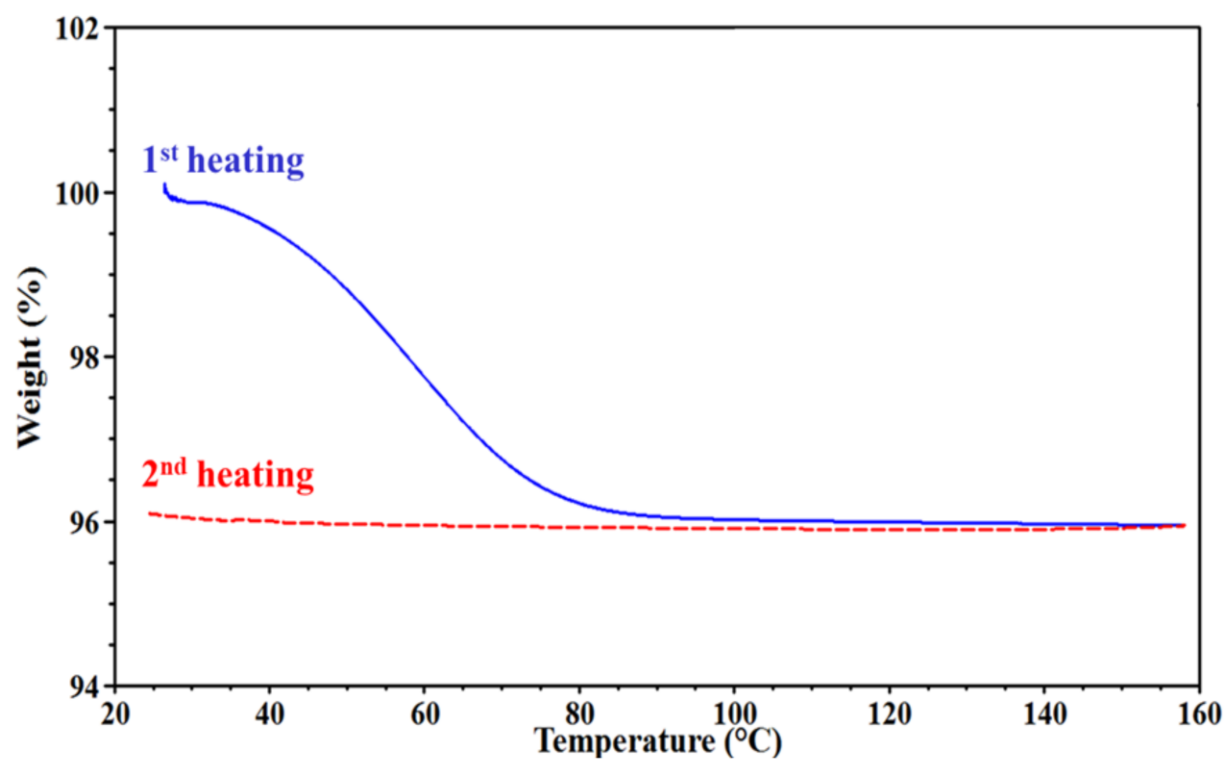
653  
654 **List of Tables**

655 **Table 3.** Summary of the results obtained for the tensile strength, percent elongation at break and  
656 elastic modulus of HPMC films with increasing PEG 400 (% w/w) content.

657 **Table 4.** Summary of the data obtained for the cooperative relaxation TSDC peak temperature  
658 ( $T_g'$ ), relaxation time ( $\tau$ ), for the highest intensity TW output, and bulk glass transition temperature  
659 ( $T_g$ ) obtained for the HPMC films.

660

661  
662  
663  
664  
665



666  
667 Figure 1  
668

669

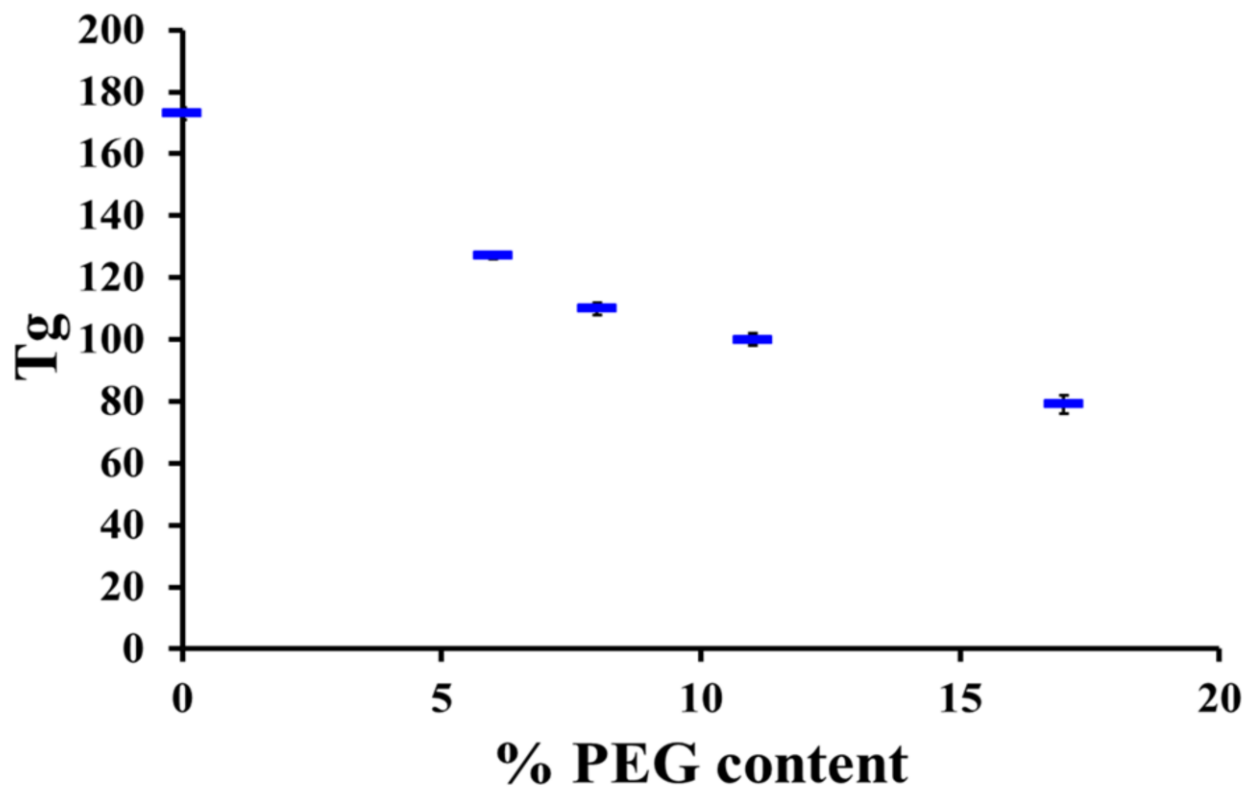
670

671

672

673

674

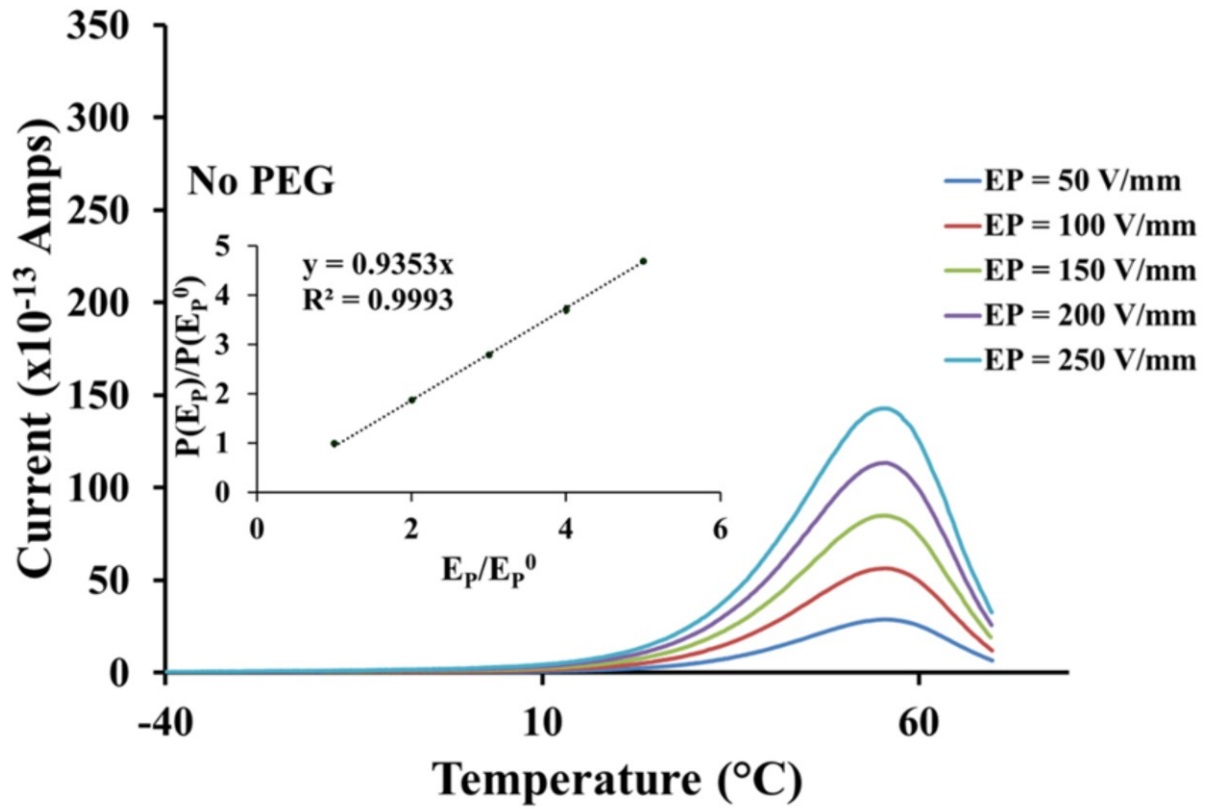


675

676 Figure 2

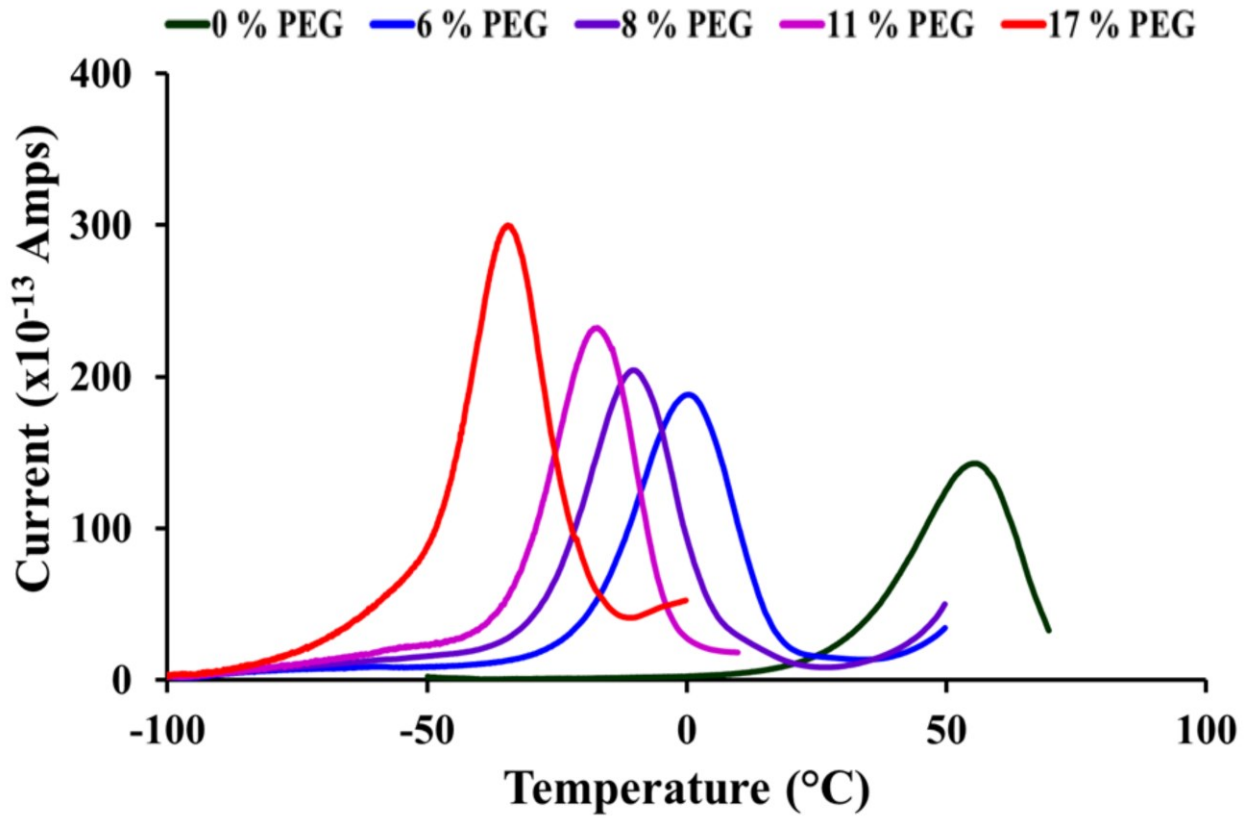
677

678  
679  
680  
681  
682  
683  
684  
685  
686



687  
688 Figure 3

689  
690  
691  
692  
693  
694  
695

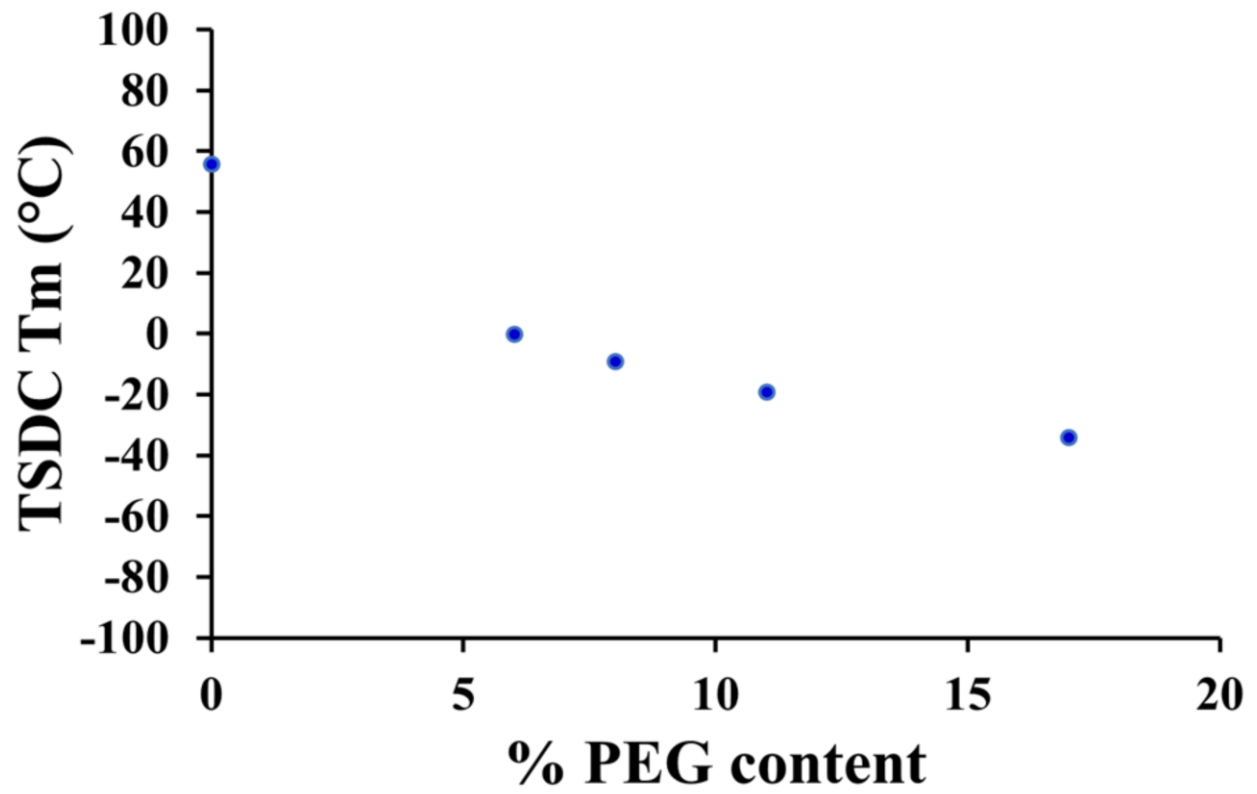


696  
697  
698

Figure 4



699  
700  
701  
702  
703  
704  
705  
706  
707



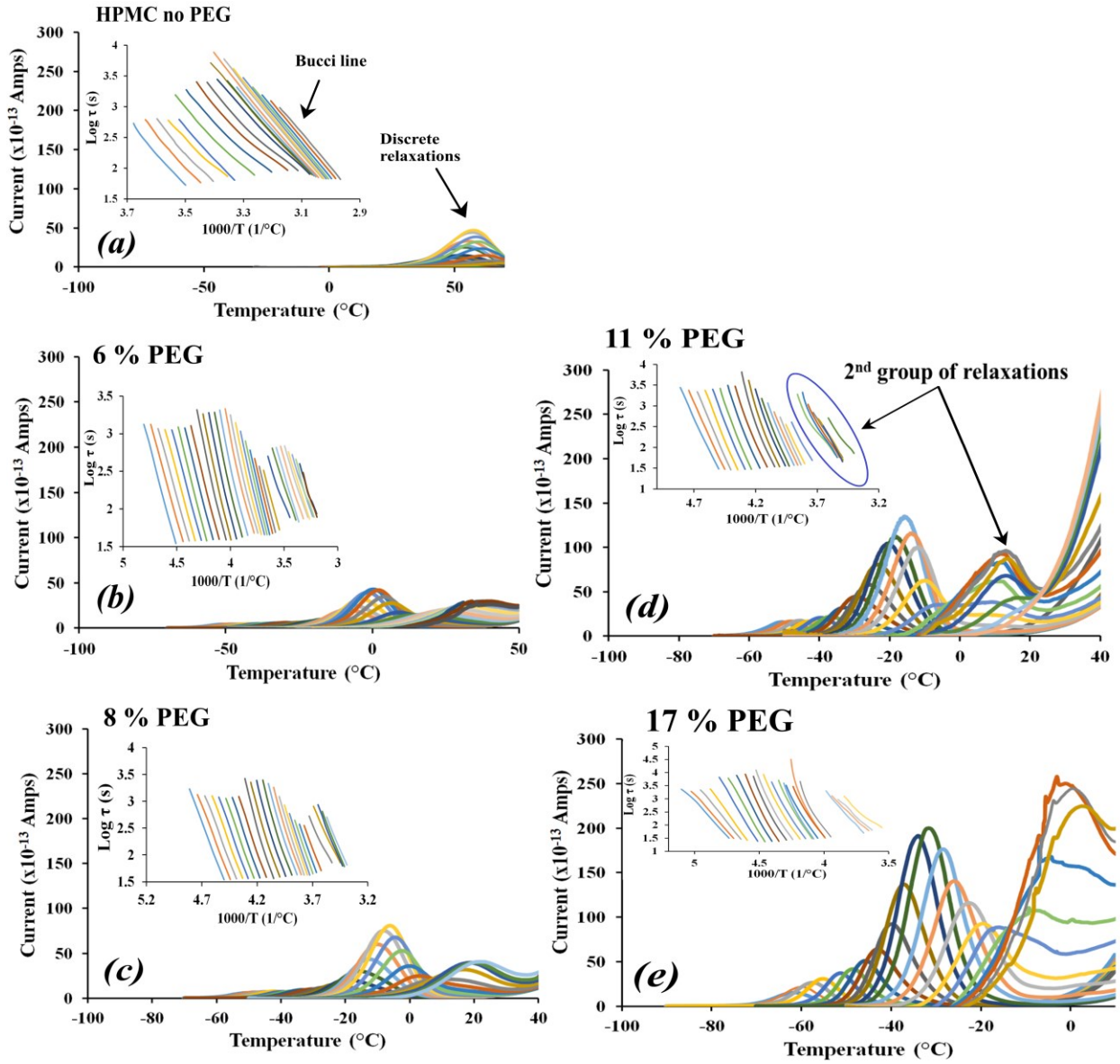
708  
709  
710

Figure 5

711

712

713



714

715 Figure 6

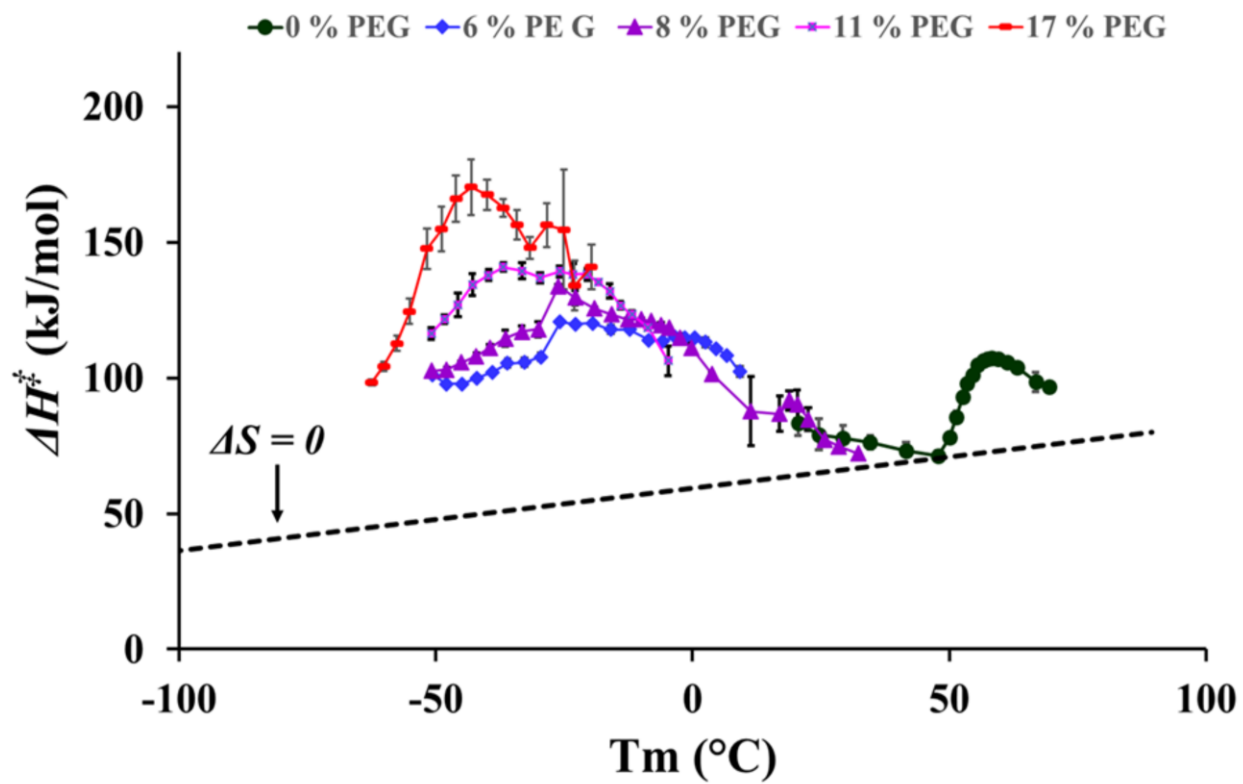
716

717

718

719

720



721

722 Figure 7

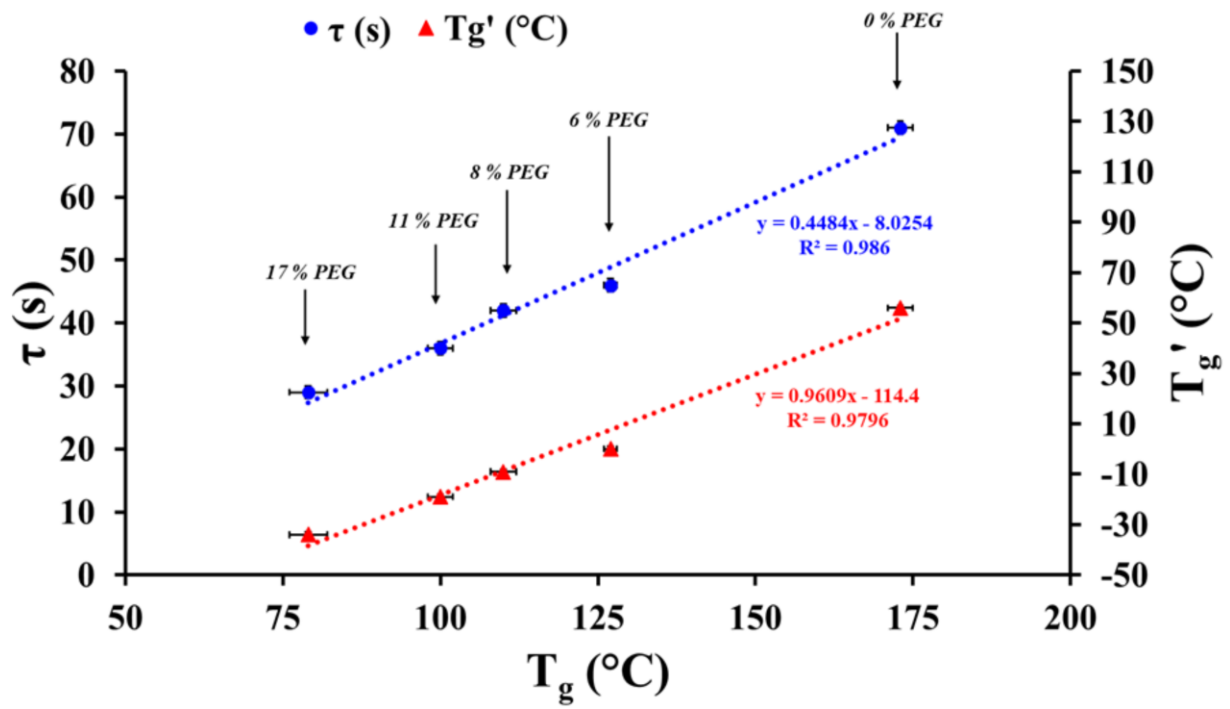
723

724

725

726

727



728

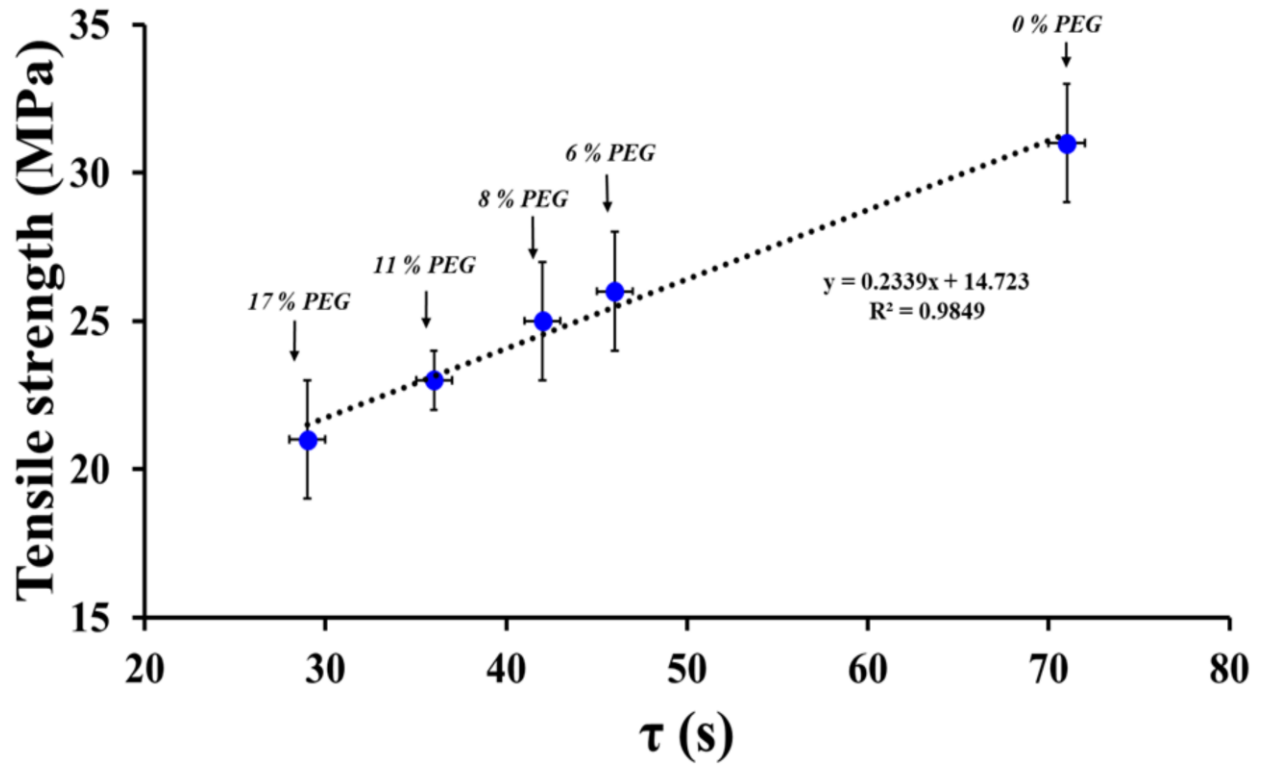
729 Figure 8

730

731

732

733



734

735 Figure 9

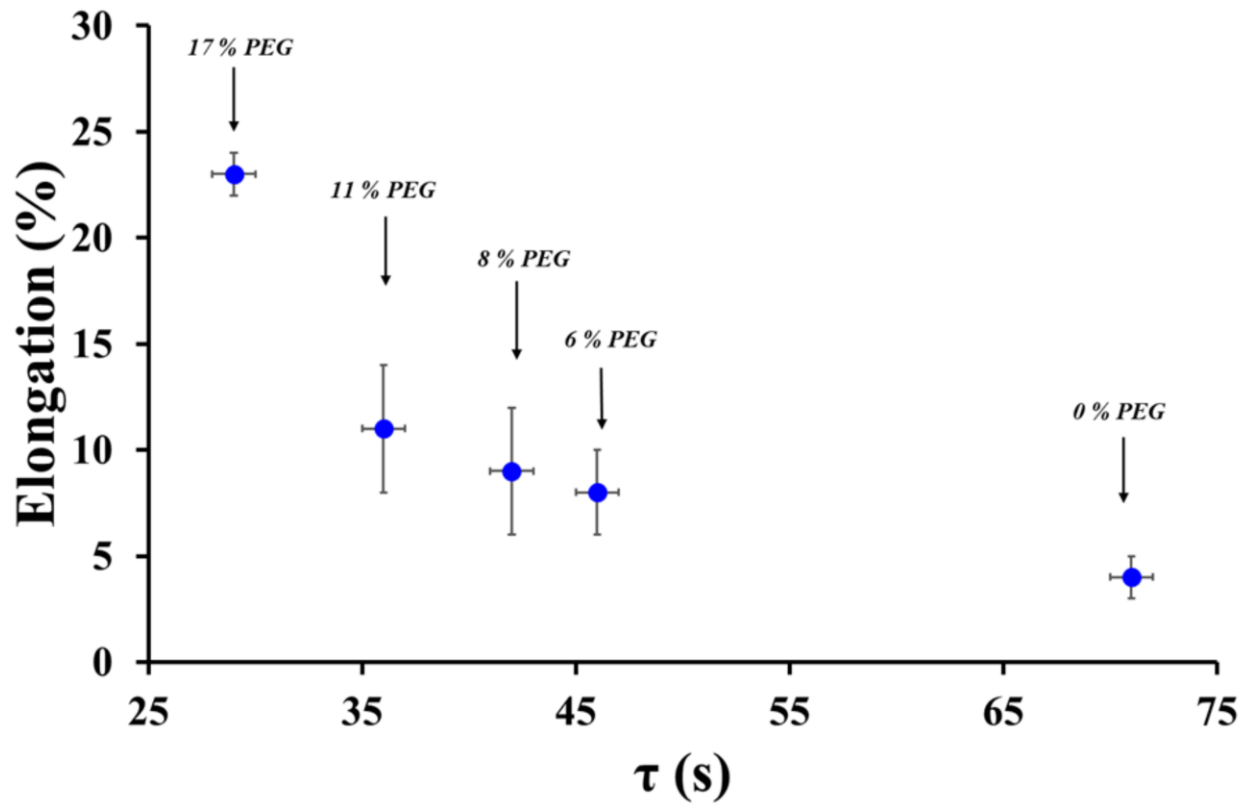
736

737

738

739

740



741

742 Figure 10

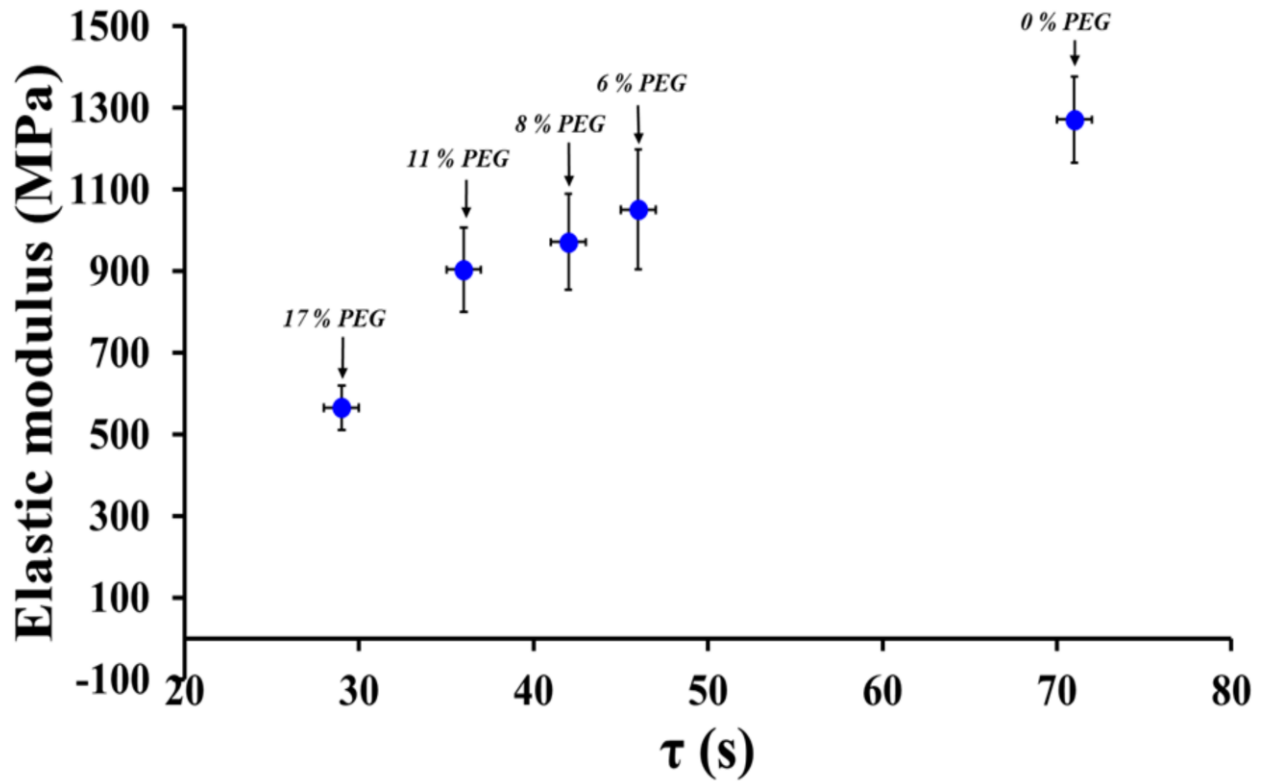
743

744

745

746

747



748

749 Figure 11